Electronic Supplementary Information

Experimental section

Materials: GO, copper sulfate ($CuSO_4$), ammonium chloride (NH_4Cl), hydrazine hydrate ($N_2H_4 \cdot H_2O$), salicylic acid ($C_7H_6O_3$), sodium citrate ($C_6H_5Na_3O_7$), sodium hypochlorite (NaClO), sodium hydroxide (NaOH), hydrochloric acid (HCl), ethanol (CH_3CH_2OH), sodium monophosphate (NaH_2PO_2) and carbon paper (CP) were bought from Beijing Chemical Corporation. Para-(dimethylamino) benzaldehyde ($C_9H_{11}NO$), sodium nitroferricyanide (III) dihydrate ($Na_2Fe(CN)_5NO \cdot 2H_2O$), and Nafion were purchased from Aladdin Ltd. (Shanghai, China). The water used throughout all experiments was purified through a Millipore system.

Preparation of Cu_3P-rGO: Aqueous solution of $CuSO_4$ (100 mL, 0.05 M) and NaOH (40 mL, 0.25 M) was dissolved in homogeneous GO aqueous dispersion (1mg/mL) under stirring for 2 h. After that, the product was separated by centrifuging, and further washing was done with Millipore water. Finally, the nanocomposite sample was freeze-dried for 24 h. The product and NaH_2PO_2 (mass ratio 1: 5) were put into two boats separately and then annealed at 300 °C for 2 h under argon flow with a ramping rate of 2 ℃ min^{-1}. In addition, Cu_3P was also prepared according to the same method only without adding GO. In addition, Cu-rGO was also prepared through annealing product at 300 ℃ for 2 h under Ar/H_2 atmosphere (volume ratio = 9:1) atmosphere without adding NaH_2PO_2.

Preparation of Cu_3P-rGO/CP electrode: 10 mg Cu_3P-rGO powders and 40 μL of Nafion solution (5 wt%) were dispersed in 960 μL mixed solution containing 720 μL ethanol and 240 μL H_2O by 2 h sonication to form a homogeneous ink. Then, 10 μL Cu_3P-rGO was loaded on a CP with area of 1 x 1 cm^2 and dried under ambient condition.

Characterizations: X-ray diffraction (XRD) analysis was performed using a LabX XRD-6100 X-ray diffractometer with Cu Kα radiation (λ = 1.5418 Å) at 40 kV and 40 mA. Scanning electron microscope (SEM) measurements were recorded on a XL30 ESEM FEG scanning electron microscope at an accelerating voltage of 20 kV.

Transmission electron microscopy (TEM) images were obtained from a Zeiss Libra 200FE transmission electron microscope operated at 200 kV. X-ray photoelectron spectroscopy (XPS) measurements were performed on an ESCALABMK II X-ray photoelectron spectrometer using Mg as the exciting source. The absorbance data of spectrophotometer were measured on SHIMADZU UV-2700 ultraviolet-visible (UV-Vis) spectrophotometer.

Electrochemical measurements: Electrochemical measurements were performed with a CHI 660E electrochemical analyzer (CH Instruments, Inc., Shanghai) using a standard three-electrode system using Cu_3P-rGO/CP loaded on carbon paper (Cu_3P-rGO/CP; Cu_3P-rGO loading: 0.1 mg cm^{-2}) as the working electrode, graphite rod as the counter electrode, and saturated Ag/AgCl electrode as the reference electrode. The potentials reported in this work were converted to reversible hydrogen electrode (RHE) scale via calibration with the following equation: E (vs. RHE) = E (vs. Ag/AgCl) + 0.059 × pH + 0.197 V. Prior to use, the electrochemical cell was immersed in 0.05 M H_2SO_4 solution for 24 h and then washed with deionized water to eliminate contaminants. In the process of electrochemical measurement, N_2 (99.999%) was firstly bubbled into 0.05 M H_2SO_4 to remove the possible NH_3, then bubbled into a Cu impurity trap, which composed of 2 g Cu-Zn-Al oxide catalyst to remove the possible NO_x contaminants, and finally bubbled up at the bottom of the cathodic compartment to saturate the 0.1 M HCl (the HCl electrolyte was purged with N_2 for 0.5 h before the measurement). All experiments were carried out at room temperature. For electrochemical N_2 reduction, chrono-amperometry tests were conducted in N_2-saturated 0.1 M HCl solution.

Determination of NH_3: The produced NH_3 was spectrophotometrically determined by the indophenol blue method.[1] In detail, 2 mL electrolyte was taken from the cathodic chamber, and then 2 mL of 1 M NaOH solution containing 5% salicylic acid and 5% sodium citrate was added into this solution. Subsequently, 1 mL of 0.05 M NaClO and 0.2 mL of 1% $C_5FeN_6Na_2O{\cdot}2H_2O$ were add into the above solution. After standing at room temperature for 2 h, UV-Vis absorption spectrum was measured at a wavelength of 655 nm. The concentration-absorbance curve was calibrated using

standard NH_4^+ solution with a serious of concentrations. The fitting curve (y = 0.432x + 0.062, R^2 = 0.999) shows good linear relation of absorbance value with NH_4^+ concentration.

Determination of N_2H_4: N_2H_4 in the electrolyte was estimated by the method of Watt and Chrisp.[2] The mixture solution of 5.99 g $C_9H_{11}NO$, 30 mL HCl and 300 mL ethanol was used as a color reagent. Typically, 5 mL electrolyte was removed from the electrochemical reaction vessel and added into 5 mL above prepared color reagent 10 min at room temperature. Moreover, the absorbance of the resulting solution was measured at a wavelength of 455 nm. The obtained calibration curve of N_2H_4 is y = 0.71x + 0.035, R^2 = 0.999.

Calculations of NH_3 yield rate and FE: NH_3 yield was calculated using the following equation:

$$NH_3 \text{ yield} = [NH_4^+] \times V/(m_{cat.} \times t)$$

FE was calculated according to following equation:

$$FE = 3 \times F \times [NH_4^+] \times V/(18 \times Q)$$

Where $[NH_4^+]$ is the measured NH_4^+ concentration; V is the volume of the cathodic reaction electrolyte; t is the potential applied time; $m_{cat.}$ is the loaded quality of catalyst; F is the Faraday constant; and Q is the quantity of applied electricity.

Details of Density Functional Theory (DFT) Calculations: Density functional theory (DFT) was carried out by the Vienna ab initio Simulation Package (VASP).[3,4] The ion-electron interactions were described by Projector augmented wave (PAW)[5] method. The generalized gradient approximation (GGA) in the Perdew-Burke-Ernzerhof (PBE) form [6,7] was employed. A cut-off energy for plane wave basis set was set to 400 eV and geometry optimizations were performed until the residual force on each atom becomes less than 0.03 eV/Å. A (3×3×1) Gamma-center mesh k-point was used for the calculation, and more than 15 Å of vacuum in z-direction was included for the slab model to avoid the interaction between two periodic units. The optimized Cu_3P (100) surface was shown in Fig. S8. The adsorption energies (E_{ads}) of the NRR intermediates were determined by $E_{ads} = E_{tot} - E_{slab} - E_{adsorbate}$, where E_{tot}, E_{slab} and $E_{adsorbate}$ represent the total energies of the species adsorbed slab system, the

clean slab, and the adsorbate, respectively. The calculations of Gibbs free energy change (ΔG) was computed by $\Delta G = \Delta E + \Delta E_{ZPE} - T\Delta S + neU$ for each step, which is based on the computational hydrogen electrode (CHE) model proposed by Nørskov e. al,[8] where ΔE is the reaction energy directly obtained from DFT computation; ΔE_{ZPE} and ΔS are the changes in zero-point energies and entropy, respectively; T is the temperature, which is set to be 298.15 K in this work; n and U are the number of electrons transferred and the applied potential, respectively. In this study, the entropies of molecules in the gas phase were obtained from the NIST database.

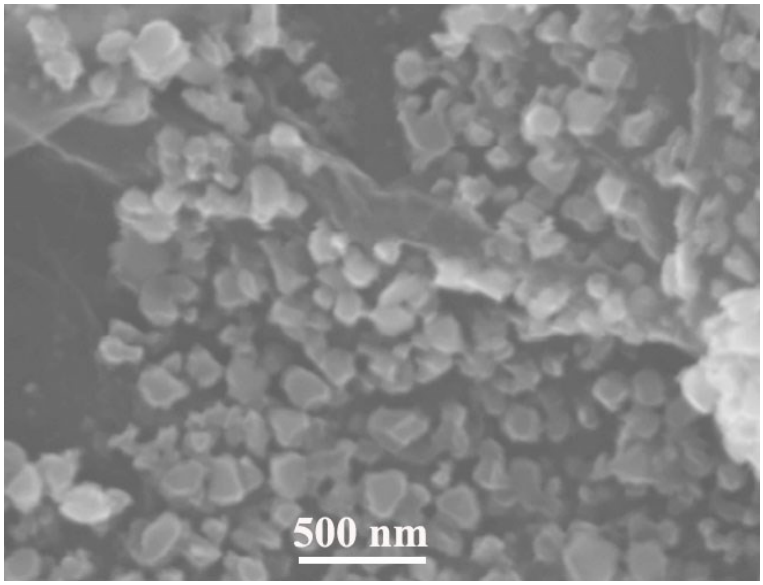

Fig. S1. SEM image of Cu_3P-rGO.

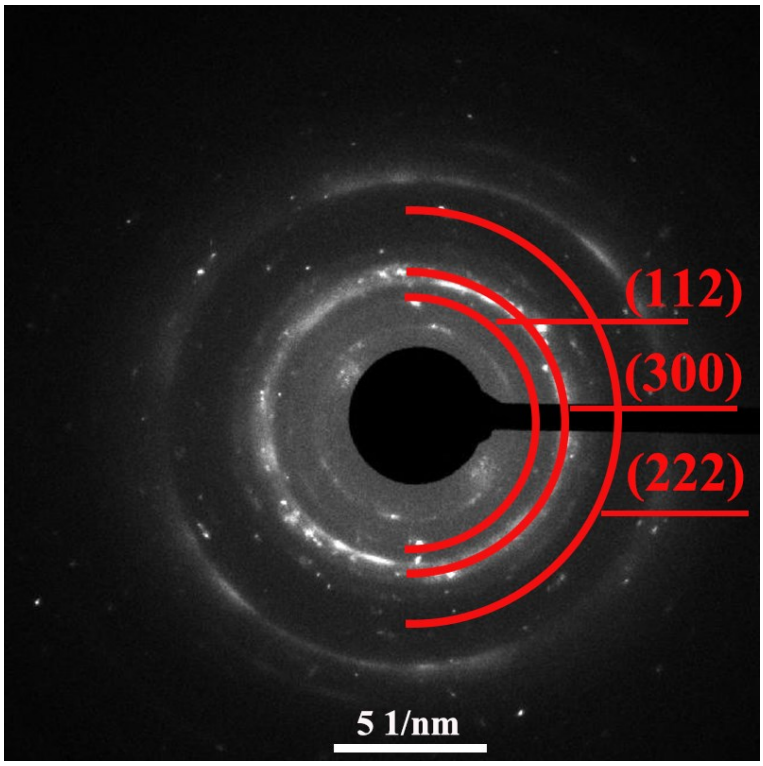

Fig. S2. SAED pattern taken from Cu_3P-rGO.

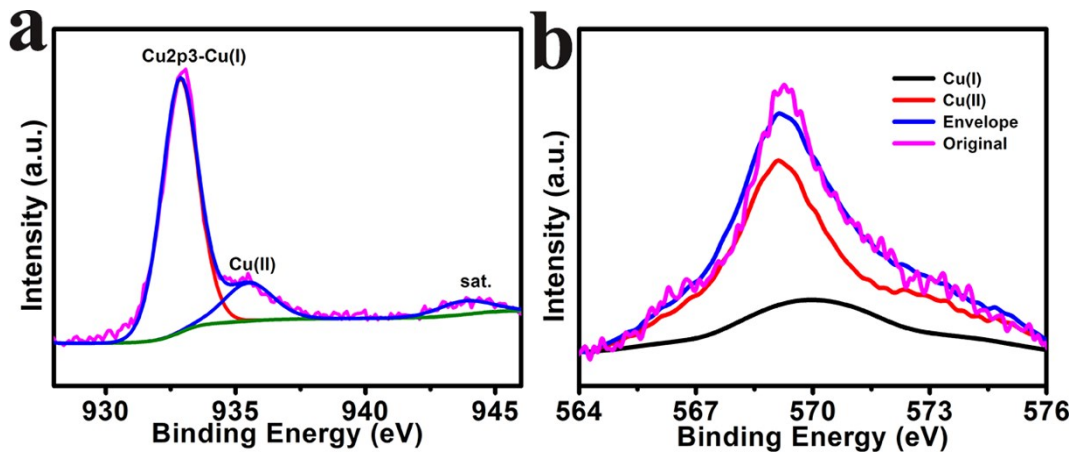

Fig. S3. (a) XPS spectrum of Cu_3P-rGO and (b) Auger electron spectrum in the Cu 2p.

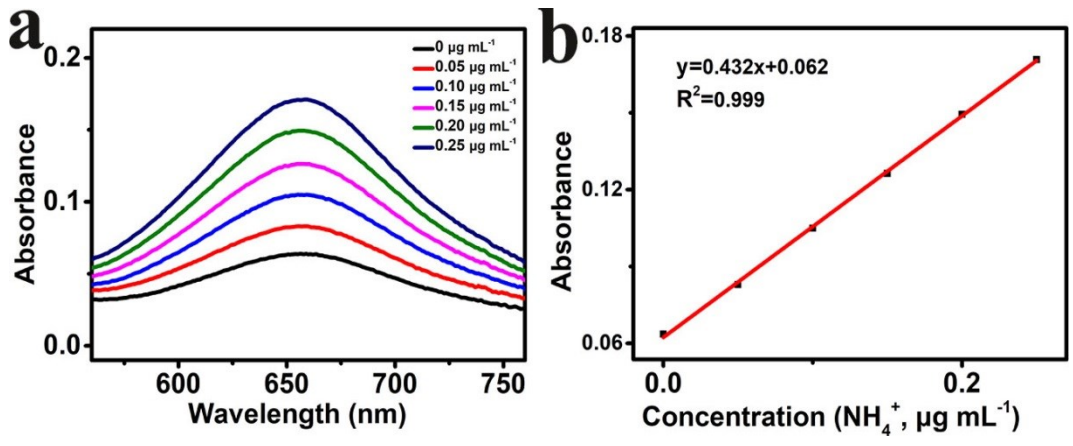

Fig. S4. (a) UV-Vis absorption spectra of indophenol assays with NH_4^+ concentrations after incubated for 2 h at room temperature. (b) Calibration curve used for calculation of NH_4^+ concentrations.

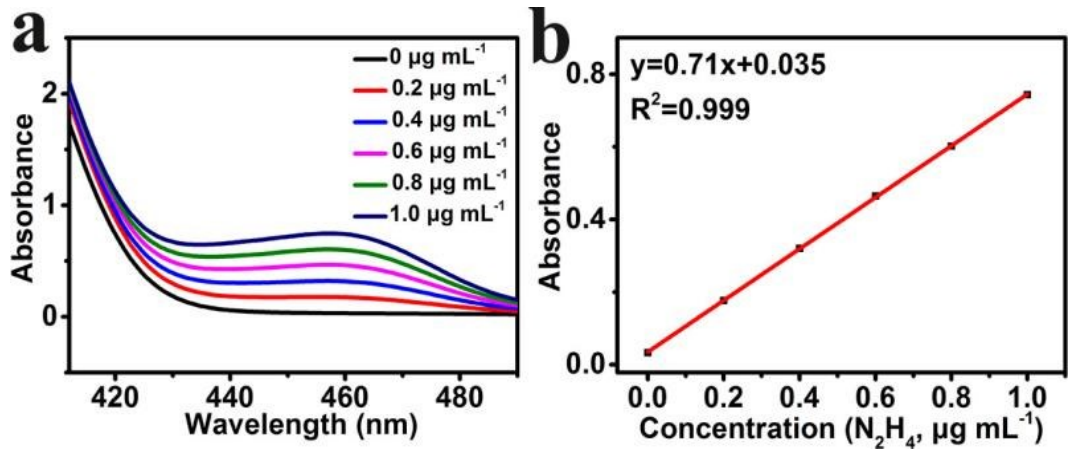

Fig. S5. (a) UV-Vis absorption spectra of various N_2H_4 concentrations after incubated for 10 min at room temperature. (b) Calibration curve used for calculation of N_2H_4 concentrations.

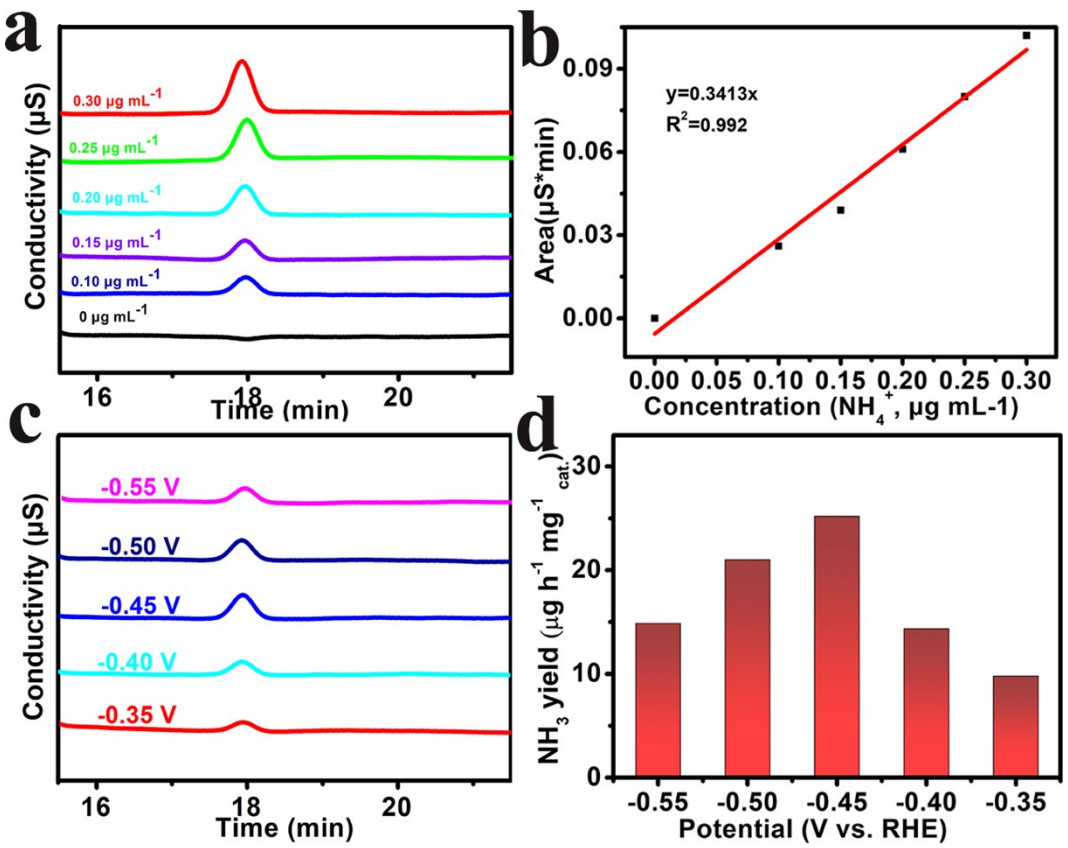

Fig. S6. (a) Ion chromatogram analysis for the NH_4^+ ions. (b) Calibration curve used for estimation of NH_4^+. (c) Ion chromatogram data for the electrolytes at a series of potentials after electrolysis for 2 h. (d) NH_3 yields for Cu_3P-rGO/CP at corresponding potentials.

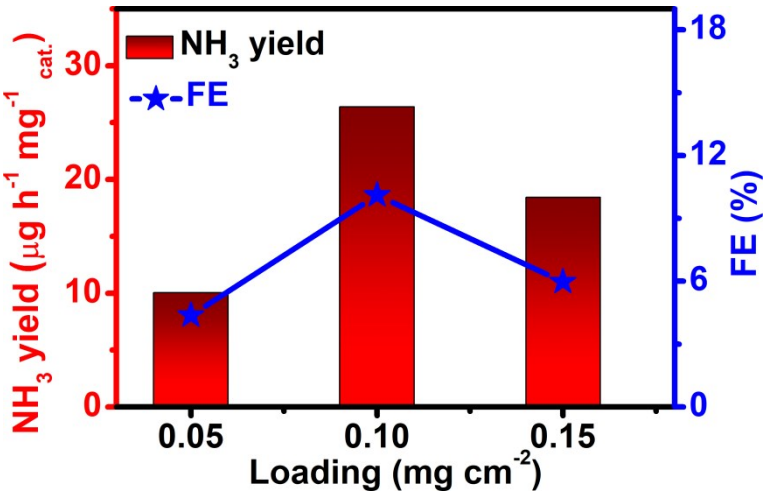

Fig. S7. NH_3 yields and FEs for Cu_3P-rGO/CP at –0.45 V with different loadings.

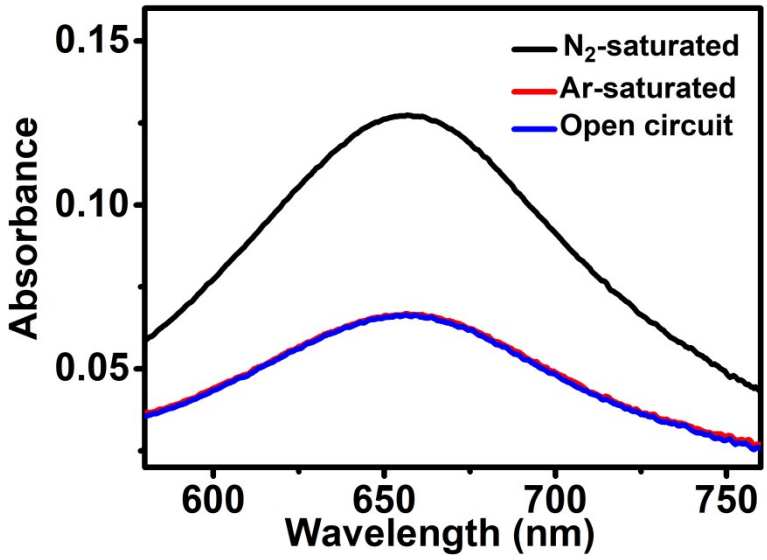

Fig. S8. UV-Vis absorption spectra of the electrolyte stained with indophenol indicator after charging at –0.45 V for 2 h under different electrochemical conditions.

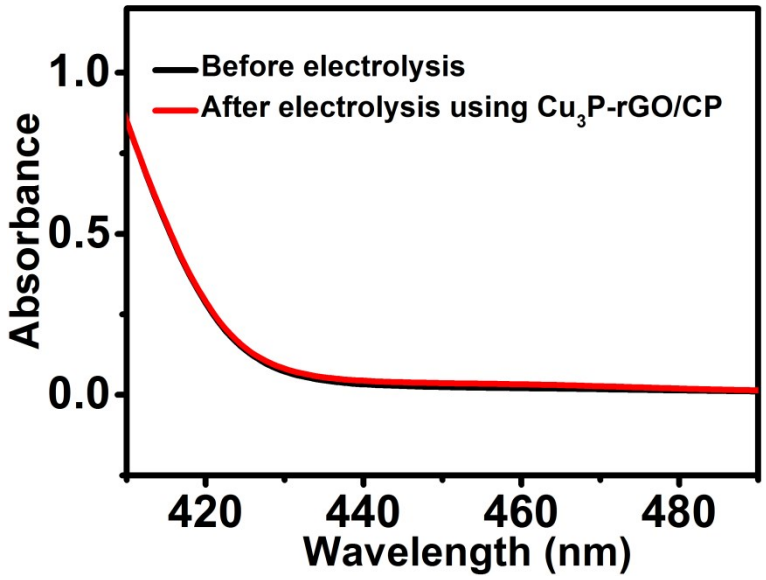

Fig. S9. UV-Vis absorption spectra of the electrolytes estimated by the method of Watt and Chrisp before and after 2 h electrolysis in N_2 atmosphere at –0.45 V.

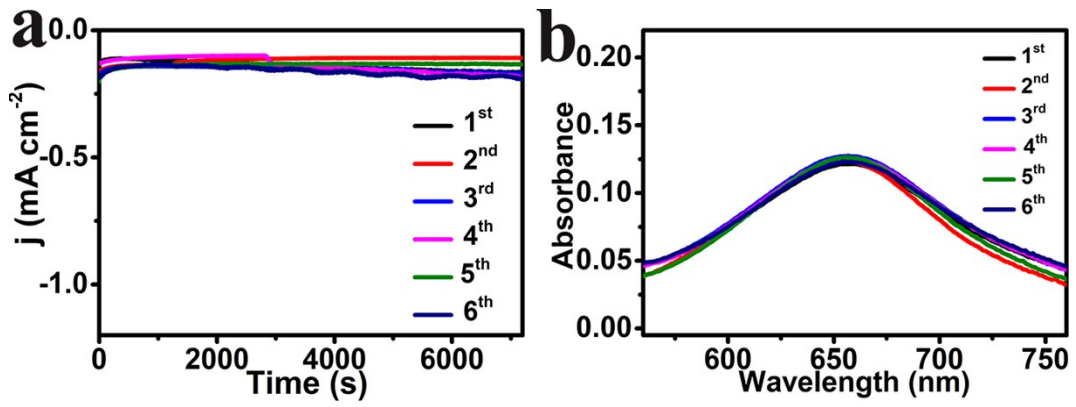

Fig. S10. (a) Time-dependent current density curves of Cu_3P-rGO/CP at –0.45 V for continuous cycles. (b) UV-Vis absorption spectra of the electrolytes stained with NH_3 color agent for continuous cycles.

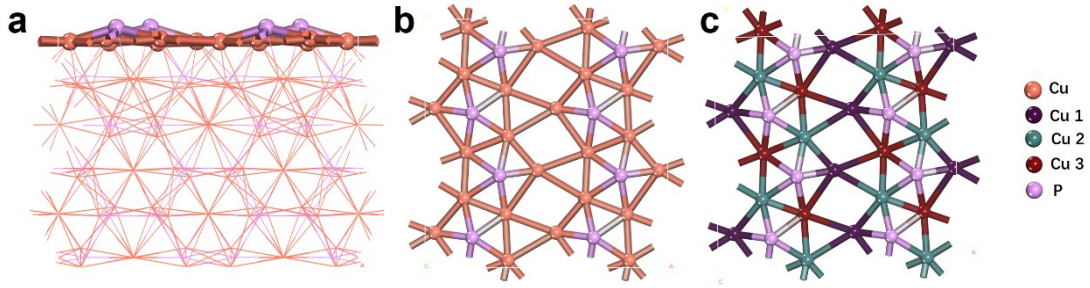

Fig. S11. Side views (a) and upper exposed surface (b-c) of the optimized Cu_3P (100) surface.

Table S1. Comparison of electrocatalytic N_2 reduction performance for Cu_3P-rGO with other aqueous-based electrocatalysts under ambient conditions.

Catalyst	Electrolyte	NH_3 yield	FE (%)	Ref.
Cu_3P-rGO	0.1 M HCl	26.38 μg h^{-1} $mg^{-1}_{cat.}$	10.11	This work
α-Au/CeO_x-RGO	0.1 M HCl	8.3 μg h^{-1} $mg^{-1}_{cat.}$	10.1	9
TA-reduced Au/TiO_2	0.1 M HCl	21.4 μg h^{-1} $mg^{-1}_{cat.}$	8.11	10
MoN NA/CC	0.1 M HCl	18.42 μg h^{-1} cm^{-2}	1.15	11
MoO_3	0.1 M HCl	29.43 μg h^{-1} $mg^{-1}_{cat.}$	1.9	12
VN/TM	0.1 M HCl	5.14 μg h^{-1} cm^{-2}	2.25	13
$Bi_4V_2O_{11}/CeO_2$	0.1 M HCl	23.21 μg h^{-1} $mg^{-1}_{cat.}$	10.16	14
Mo_2N	0.1 M HCl	78.4 μg h^{-1} $mg^{-1}_{cat.}$	4.5	15
NPC	0.05 M H_2SO_4	23.8 μg h^{-1} $mg^{-1}_{cat.}$	1.42	16
Mo nanofilm	0.01 M H_2SO_4	1.89 μg h^{-1} cm^{-2}	0.72	17
$Pd_{0.2}Cu_{0.8}$/rGO	0.1 M KOH	2.8 μg h^{-1} $mg^{-1}_{cat.}$	4.5	18
Ru/C	2.0 M KOH	0.21 μg h^{-1} cm^{-2}	0.28	19
γ-Fe_2O_3	0.1 M KOH	0.212 μg h^{-1} $mg^{-1}_{cat.}$	1.9	20
Fe_2O_3-CNT	$KHCO_3$	0.22 μg h^{-1} cm^{-2}	0.15	21
CuO/RGO	0.1 M Na_2SO_4	11.02 μg h^{-1} cm^{-2}	3.9	22
TiO_2-rGO	0.1 M Na_2SO_4	15.13 μg h^{-1} $mg^{-1}_{cat.}$	3.3	23
Fe_2O_3 nanorods	0.1 M Na_2SO_4	15.9 μg h^{-1} $mg^{-1}_{cat.}$	0.94	24
dendritic Cu	0.1 M HCl	25.63 μg h^{-1} $mg^{-1}_{cat.}$	15.12	25

References

1 D. Zhu, L. Zhang, R. E. Ruther and R. J. Hamers, *Nat. Mater.*, 2013, **12**, 836–841.

2 G. W. Watt and J. D. Chrisp, *Anal. Chem.*, 1952, **24**, 2006–2008.

3 G. Kresse and J. Furthmüller, *Phys. Rev. B*, 1996, **54**, 11169.

4 G. Kresse and D. Joubert, *Phys. Rev. B*, 1999, **59**, 1758.

5 P. E. Blöchl, *Phys. Rev. B*, 1994, **50**, 17953.

6 J. P. Perdew, J. Chevary, S. Vosko, K. A. Jackson, M. R. Pederson, D. Singh and C. Fiolhais, *Phys. Rev. B,* 1992, **46**, 6671.

7 J. P. Perdew and Y. Wang, *Phys. Rev. B*, 1992, **45**, 13244.

8 A. A. Peterson, F. Abild-Pedersen, F. Studt, J. Rossmeisl and J. K. Nørskov, *Energy Environ. Sci.,* 2010, **3**, 1311–1315.

9 S. Li, D. Bao, M. Shi, B. Wulan, J. Yan and Q. Jiang, *Adv. Mater.*, 2017, **29**, 1700001.

10 M. Shi, D. Bao, B. Wulan, Y. Li, Y. Zhang, J. Yan and Q. Jiang, *Adv. Mater.*, 2017, **29**, 1606550.

11 L. Zhang, X. Ji, X. Ren, Y. Luo, X. Shi, A. M. Asiri, B. Zheng and X. Sun, *ACS Sustainable Chem. Eng.*, 2018, **6**, 9550–9554.

12 J. Han, X. Ji, X. Ren, G. Cui, L. Li, F. Xie, H. Wang, B. Li and X. Sun, *J. Mater. Chem. A*, 2018, **6**, 12974–12977.

13 R. Zhang, Y. Zhang, X. Ren, G. Cui, A. M. Asiri, B. Zheng and X. Sun, *ACS Sustainable Chem. Eng.*, 2018, **6**, 9545–9549.

14 C. Lv, C. Yan, G. Chen, Y. Ding, J. Sun, Y. Zhou and G. Yu, *Angew. Chem., Int. Ed.*, 2018, **57**, 6073–6076.

15 X. Ren, G. Cui, L. Chen, F. Xie, Q. Wei, Z. Tian and X. Sun, *Chem. Commun.*, 2018, **54**, 8474–8477.

16 Y. Liu, Y. Su, X. Quan, X. Fan, S. Chen, H. Yu, H. Zhao, Y. Zhang and J. Zhao, *ACS Catal.*, 2018, **8**, 1186–1191.

17 D. Yang, T. Chen and Z. Wang, *J. Mater. Chem. A*, 2017, **5**, 18967–18971.

18 M. Shi, D. Bao, S. Li, B. Wulan, J. Yan and Q. Jiang, *Adv. Energy Mater.,* 2018, **8**, 1800124.

19 V. Kordali, G. Kyriacou and C. Lambrou, *Chem. Commun*., 2000, **17**, 1673–1674.

20 J. Kong, A. Lim, C. Yoon, J. H. Jang, H. C. Ham, J. Han, S. Nam, D. Kim, Y. E. Sung, J. Choi and H. S. Park, *ACS Sustainable Chem. Eng.*, 2017, **5**, 10986–10995.

21 S. Chen, S. Perathoner, C. Ampelli, C. Mebrahtu, D. Su and G. Centi, *Angew. Chem., Int. Ed.*, 2017, **56**, 2699–2703.

22 F. Wang, Y. Liu, H. Zhang and K. Chu, *ChemCatChem*, 2019, **11**, 1441–1447.

23 X. Zhang, Q. Liu, X. Shi, A. M. Asiri, Y. Luo, X. Sun and T. Li, *J. Mater. Chem. A*, 2018, **6**, 17303–17306.

24 X. Xiang, Z. Wang, X. Shi, M. Fan and X. Sun, *ChemCatChem*, 2018, **10**, 4530–4535.

25 C. Li, S. Mou, X. Zhu, F. Wang, Y. Wang, Y. Qiao, X. Shi, Y. Luo, B. Zheng, Q. Li and X. Sun, *Chem. Commun.*, 2019, **55**, 14474–14477.